Journal of Solid State Chemistry 182 (2009) 597–601

Contents lists available at ScienceDirect

Journal of Solid State Chemistry

journal homepage: www.elsevier.com/locate/jssc

Synthesis of highly fluorescent LaF_3:Ln^{3+}/LaF_3 core/shell nanocrystals by a surfactant-free aqueous solution route

Meng-Yin Xie, Liao Yu, Hui He, Xue-Feng Yu *

Department of Physics, Key Laboratory of Acoustic and Photonic Materials and Devices of Ministry of Education, Wuhan University, Wuhan 430072, People's Republic of China

ARTICLE INFO

Article history:
Received 1 July 2008
Received in revised form
2 November 2008
Accepted 14 December 2008
Available online 24 December 2008

Keywords:
LaF_3
Nanocrystals
Core/shell
Quantum yield

ABSTRACT

A surfactant-free aqueous solution route has been established for the synthesis of LaF_3:Ln^{3+}/LaF_3 core/shell nanocrystals (Ln = Ce, Tb, Nd) heated at 75 °C at ambient pressure. All the as-prepared nanocrystals with spherical shape have an average size around 20 nm, and consist of well crystallized hexagonal phases. The X-ray photoelectron spectra was used to confirm that the LaF_3 shells have coated the LaF_3:Ce^{3+}, Tb^{3+} cores. Compared with that of the original cores under the same conditions, the emission intensity of the LaF_3:Ce^{3+}, Tb^{3+}/LaF_3 and LaF_3:Nd^{3+}/LaF_3 core/shell nanocrystals increased significantly of 120% and 60%, respectively. The quantum yield of the LaF_3:Ce^{3+}, Tb^{3+}/LaF_3 core/shell nanocrystals reached about 27% in aqueous solution. These results indicate that a significant reduction of the quenching from the surface of the core nanocrystals can be obtained by the synthesis of the core/shell structures, and this method can provide more desirable lanthanide-doped nanocrystals for potential biological applications.

1. Introduction

The past 10 years have witnessed a great increase in research on inorganic fluorescent nanocrystals (NCs). Especially semiconductor quantum dots (QDs) whose light emission is influenced by quantum confinement effects have attracted much attention of scientists [1–5]. For increasing the fluorescence efficiency of the QDs, strategies were developed to synthesize core/shell structures to suppress energy-loss processes at the particle surface [1,2]. As a result, the core/shell structured QDs, providing higher quantum efficiency than organic dyes, have been widely used in biological areas [3–7]. However, QDs were still controversial in biological areas because of their inherent toxicity and chemical instability [8]. Recently, lanthanide-doped NCs aroused peoples' interests significantly as fluorescent labeling alternatives to QDs, considering their attractive chemical and optical features such as low toxicity, characteristic narrow emission, and excellent photostability [9–15]. The synthesis of core/shell structures is an effective solution to suppress the surface quenching and increase the quantum yield of the lanthanide-doped NCs, as of the QDs. Currently, the synthesis of the core/shell structured NCs by using different passivating inorganic shells (such as un-doped $LaPO_4$, LaF_3 and $NaYF_4$) to cap lanthanide-doped cores has been reported by several groups [16–25]. In these works, the materials with similar lattice constants as lanthanide-doped cores were chosen as the shells to avoid the formation of defects at the core–shell interface.

Fluorides are more attractive as fluorescent host materials than traditional oxide-based systems, such as Y_2O_3, $LaPO_4$ and YVO_4, owing to their low vibrational energies, and the subsequent minimization of the quenching of the excited state of the lanthanide ions [15]. Hence, many efforts have focused on $NaYF_4$ and LaF_3 as lanthanide-doped hosts in recent years. $NaYF_4$ as the hexagonal phase is the most efficient upconversion host material known to date [13,14]. However, high temperature must be employed in the synthesis of hexagonal $NaYF_4$. LaF_3 are often chosen as the host for downconverison ions, such as Ce^{3+}, Tb^{3+} and Nd^{3+}. It has very low vibrational energy due to the high ionicity of the La^{3+} to fluorine bond, therefore its non-radiative loss is suppressed and a high quantum efficiency of the desired luminescence can be obtained [12,15].

Water-soluble lanthanide-doped NCs were demonstrated to be more preferable for bio-applications [10]. Organic surfactants were often used in the synthesis to render LaF_3 NCs water-soluble and control their size; however, they also quenched the fluorescence. In 2006, Wang et al. developed a facile method to synthesize LaF_3:Ln^{3+} NCs directly in water without any organic surfactant, but a relatively low quantum yield was found. In this paper, we reported a surfactant-free aqueous solution route to synthesize highly fluorescent LaF_3:Ln^{3+}/LaF_3 core/shell NCs at a low temperature of 75 °C at ambient pressure, and the products could be dispersed well in water. Various lanthanide ions Ce^{3+}, $Tb^{3+,}$ and Nd^{3+}) with fluorescence from the visible (VIS) to near-infrared (NIR) region were doped into, and the un-doped

---

* Corresponding author. Fax: +86 27 6875 2569.
E-mail address: yxf@whu.edu.cn (X.-F. Yu).

0022-4596/$ - see front matter © 2008 Elsevier Inc. All rights reserved.
doi:10.1016/j.jssc.2008.12.011

LaF_3 shell were used as the outer layer. Their structure characterization and fluorescent properties were studied, and a huge increase of fluorescence intensity and a quantum yield of about 27% were found.

2. Experimental

Lanthanide chlorides and ammonium fluoride were purchased from Sigma-Aldrich (St. Louis, MO, USA) and used as received. Lanthanide chlorides stock solutions (0.2 M) and ammonium fluoride stock solutions (0.6 M) were prepared by dissolving in deionized (DI) water.

LaF_3:Ln^{3+} NCs with a narrow size distribution were prepared by modifying the method reported by Wang et al. [15]. A mixed aqueous solution of Ln^{3+} (3.2 ml $LaCl_3$, 3.6 ml $CeCl_3$, 1.2 ml $TbCl_3$ or 7.6 ml $LaCl_3$, 0.4 ml $NdCl_3$) were added to 32 ml DI water under continue stirring for 10 min, and heated to 75 °C. Then 10 ml NH_4F was added into and the mixture was kept at 75 °C for 2 h at ambient pressure under continue stirring. The obtained NCs were collected by centrifugation at 6,000 rpm for 5 min. The crude precipitate was then re-suspended in DI water and centrifuged at 10,000 rpm for 15 min. The washing procedure was repeated three times and then the NCs were stored in 1 ml DI water. Powders of the NCs were obtained from the colloidal solution by centrifuging and subsequently drying under vacuum at ambient temperature.

LaF_3:Ln^{3+}/LaF_3 core/shell NCs were prepared by using the following method. A mixed aqueous solution of 0.2 ml as-prepared LaF_3:Ln^{3+} NCs were divided into two parts. One part (0.1 ml) of the LaF_3:Ln^{3+} NCs and 0.2 ml $LaCl_3$ were added to 3.7 ml DI water under continue stirring for 10 min, and heated to 75 °C. Then, 0.2 ml NH_4F was added into and the mixture was kept at 75 °C for 2 h at ambient pressure under continue stirring. The obtained NCs were collected by centrifugation at 6,000 rpm for 5 min. Then the core/shell NCs were stored in 1 ml DI water. Another part (0.1 ml) of the LaF_3:Ln^{3+} NCs were mixed together with 0.9 ml DI water under ultrasonication and kept for 10 min. These two samples were prepared for the comparison of the fluorescence intensity.

The transmission electron microscopy (TEM) image and the high resolution TEM (HRTEM) image were measured with a JEOL 2010 HT and a JEOL 2010 FET transmission electron microscope (operated at 200 kV). Powder X-ray diffraction (XRD) analyses were performed on a Bruker D8-advance X-ray diffractometer with Cu$K\alpha$ irradiation ($\lambda = 1.5406$ Å) at a scanning speed of 0.025°/s over the 2θ range of 20°–70°. X-ray photoelectron spectra (XPS) were taken on a Kratos Ltd. XSAM800 electron energy spectrometer. The fluorescence excitation and emission spectra of were obtained with a Hitachi F-4500 fluorescence spectrophotometer. The excitation source for the fluorescence spectra of Nd^{3+} ions in the NIR region was a Ti:Sapphire CW laser (Mira 900, Coherent) with tunable wavelength in the range 700–1000 nm. The fluorescence spectra were recorded by a spectrometer (Spectrapro 2500i, Acton) with liquid nitrogen cooled CCD (SPEC-10:100B, Princeton) and corrected with the spectroscopy quantum efficiency curves.

3. Results and discussion

Fig. 1 (a) and (b) show the TEM images of the well-separated spherical shaped LaF_3:Ce^{3+}, $Tb^{3+}$and LaF_3:Ce^{3+}, Tb^{3+}/LaF_3 core/shell NCs, respectively. The high degree of dispersibility may indicate that the surface of the NCs is covered by hydroxyl groups, which limit the growth of the particles and stabilize them against agglomeration [15]. The average diameter of the LaF_3:Ce^{3+}, Tb^{3+} is around 20 nm, after coating with the LaF_3 shells, the average diameter increase a little. These results are in good agreement with the calculated value using the Scherrer equation from the following XRD patterns. Fig. 1(c) shows a HRTEM image of an individual LaF_3:Ce^{3+}, Tb^{3+}/LaF_3 core/shell NC, giving the resolved lattice fringes. The inset of Fig. 1(c) displays SAED patterns taken from an individual NC, suggests that this NC was single crystalline in nature. In TEM images, contrast depends on the electron scattering power of the object forming the images. The electron scattering power in turn depends on the electron density inside the object. Hence, direct evidence can be obtained from the image contrast for the core/shell structure with different lattice parameters. For YF_3/SiO_2 core/shell structures reported previously, one can clearly observe the core/shell border from TEM images [26], however, for the LaF_3:Ce, Tb/LaF_3 core/shell NCs, no clear border could be found from the TEM images, even HRTEM images, because LaF_3 and CeF_3 have the similar lattice parameters [17].

Fig. 2 shows the XRD patterns of the LaF_3:Ce^{3+}, Tb^{3+} and LaF_3:Ce^{3+}, Tb^{3+}/LaF_3 core/shell NCs. Both two types of the NCs crystallized well and had hexagonal phase structures. The XRD patterns of the LaF_3:Ce^{3+}, Tb^{3+} NCs are in good agreement with hexagonal phase structure known from the bulk CeF_3 crystal (JCPDS Card 08-0045) due to the main amount of Ce^{3+} (45%) in the lanthanide ions. For CdSe/CdS core/shell structures, with the growth of CdS shells, diffraction peaks shift to larger angles because of the smaller lattice constant for CdS compared with CdSe [27]. It is noteworthy that for our core/shell NCs, diffraction peaks shift slightly towards patterns of LaF_3 (JCPDS Card 32-0483), a little smaller angles, and the lattice constant of LaF_3 is larger than of CeF_3. The results imply that the LaF_3 shell had formatted around the LaF_3:Ce^{3+}, Tb^{3+} cores. In Fig. 2, diffraction peaks of two samples were broadened due to the smaller crystallite size [17]. Estimated average crystallite sizes of the LaF_3:Ce^{3+}, Tb^{3+} and LaF_3:Ce^{3+}, Tb^{3+}/LaF_3 core/shell NCs are about 20 and 23 nm from the Scherrer equation, respectively.

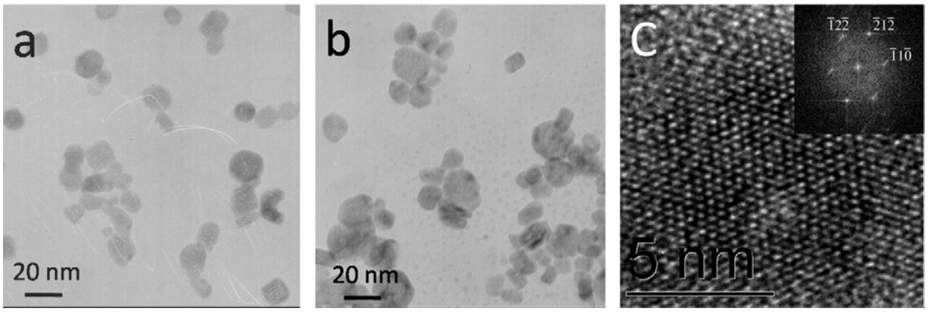

Fig. 1. Typical TEM images of LaF_3:Ce^{3+}, Tb^{3+} NCs (a), LaF_3:Ce^{3+}, Tb^{3+}/LaF_3 core/shell NCs (b) and (c) HRTEM image of one LaF_3:Ce^{3+}, Tb^{3+}/LaF_3 NC and the corresponding SAED patterns (inset).

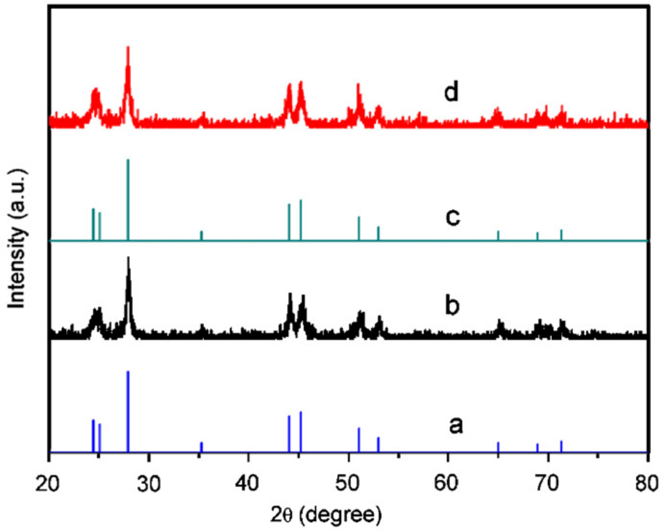

Fig. 2. XRD patterns of LaF_3:Ce^{3+}, Tb^{3+} NCs (b) and LaF_3:Ce^{3+}, Tb^{3+}/LaF_3 core/shell NCs (d); the standard data for CeF_3 (a) and LaF_3 (c).

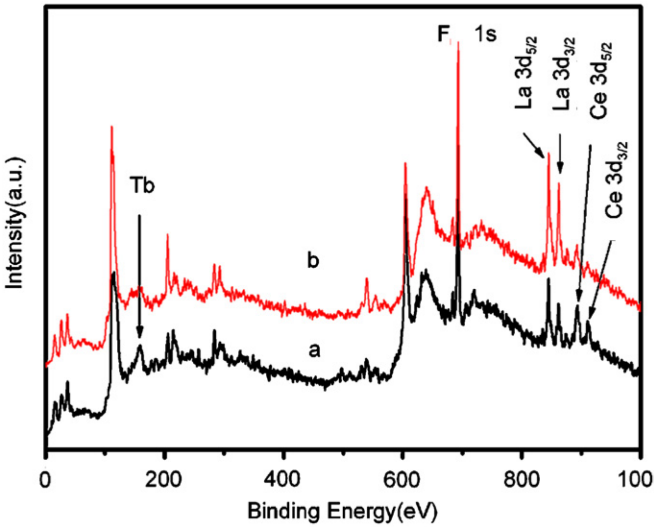

Fig. 3. XPS spectra of LaF_3:Ce^{3+}, Tb^{3+} NCs (a) and LaF_3:Ce^{3+}, Tb^{3+}/LaF_3 core/shell NCs (b).

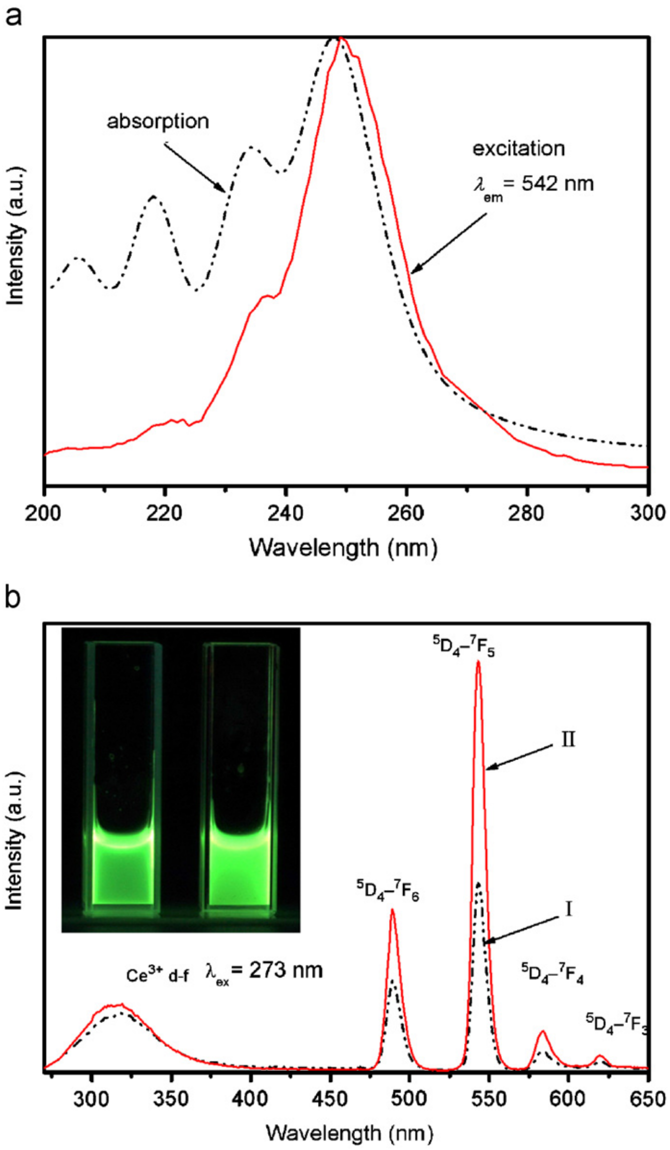

Fig. 4. (a) Absorption and excitation spectra of LaF_3:Ce^{3+}, Tb^{3+}/LaF_3 core/shell NCs; (b) emission spectra of LaF_3:Ce^{3+}, Tb^{3+} NCs (I) and LaF_3:Ce^{3+}, Tb^{3+}/LaF_3 core/shell NCs (II); Inset: photographs showing green fluorescence from these two samples.

X-ray photoelectron spectra (XPS) are well known to analyze surface elements of samples, and can penetrate only to a depth of 1–5 nm. For our core/shell NCs, XPS should be a proper method to confirm the growth of LaF_3 shells around the cores, because the mean thickness of LaF_3 shells is around 1.5 nm concluded from XRD patterns. Fig. 3 shows the XPS spectra of the LaF_3:Ce^{3+}, Tb^{3+} (a) and LaF_3:Ce^{3+}, Tb^{3+}/LaF_3 core/shell (b) NCs. The spectrum of the LaF_3:Ce^{3+}, Tb^{3+} NCs shows clear presences of visible Ce 3d (binding energy = 884.2, 902.5 eV), La 3*d* (binding energy = 837.1, 853.7 eV) and Tb (binding energy = 150.9 eV) peaks. While it is difficult to detect peaks of Ce and Tb in the XPS spectrum of LaF_3:Ce^{3+}, Tb^{3+}/LaF_3 core/shell NCs, and the peak of La is much stronger than coated before. These results indicate that the LaF_3 shells have completely covered the LaF_3:Ce^{3+}, Tb^{3+} cores. We note that only the XPS results can give the direct experimental evidence for the core/shell structure here. Since the core and shell are both based on the LaF_3 host, almost no obvious difference can be found in the TEM images or XRD spectra. Similar phenomenon has been found in previous literatures about CeF_3/LaF_3 [17] $NaYF_4$:Yb, Er/$NaYF_4$ [22] and $CePO_4$:Tb/$LaPO_4$ [28] core/shell structures.

To improve the luminescent properties of the Tb^{3+} ions in the LaF_3 host, the Ce^{3}+ and Tb^{3+} were co-doped into the LaF_3 NCs, in which the Ce^{3+} absorbs energy effectively from ultraviolet (UV) light and transfers it to the Tb^{3+} that emits green light. Under a 254 nm UV lamp irradiation, both these two NCs dispersed in water exhibited bright green emissions (inset in Fig. 4b). Fig. 4a shows the absorption and excitation spectra of the LaF_3:Ce^{3+}, Tb^{3+}/LaF_3 core/shell NCs, respectively. Monitored with the emission wavelength of 542 nm, excitation spectrum consists of a broad and strong band with a peak at 249 nm, which corresponds to the transitions from the ground state $^2F_{5/2}$ of Ce^{3+} to different components of the excited Ce^{3+} 5*d* states split by the crystal field [29]. The UV–VIS absorption spectrum of the LaF_3:Ce^{3+}, Tb^{3+}/LaF_3 core/shell NCs show four well-resolved absorption peaks at 248, 236, 218, and 208 nm for the Ce^{3+}, basically in agreement with the excitation spectrum (note that peaks at 236, 218, and 208 nm also seem to exist in the excitation spectrum evidenced by the stronger noise signals there). As a result, to get the emission spectra of these two NCs at the same excitation wavelength, the 249 nm light should be used to excite the samples.

Fig. 4b shows the emission spectra of the $LaF_3:Ce^{3+}$, Tb^{3+} and $LaF_3:Ce^{3+}$, Tb^{3+}/LaF_3 core/shell NCs in dilute water solutions. The spectra of these two samples are similar in profile, consisting of the characteristic emission of Tb^{3+} with the $^5D_4$–^7F_J ($J = 6$–3) transitions ranging from 475 to 650 nm and the characteristic emission of Ce^{3+} between 300 and 400 nm due to the 5*d*–4*f* transition. When the $LaF_3:Ce^{3+}$, Tb^{3+} NCs were coated with LaF_3 shells, the emission intensity was increased by about 120%. The significant increase of the fluorescence can be attributed to the beneficial influences of the LaF_3 shells. To further research effects of LaF_3 shells on luminescent properties of $LaF_3:Ce^{3+}$, Tb^{3+} cores, we measured quantum yields of both two samples. Commonly, the quantum yield of luminous material was determined by comparison with a dye. In this experiment, quinine bisulfate in 0.5 M H_2SO_4 was chosen as the standard because this dye is more suitable for excitation in the UV light [30]. The quantum yield was calculated from the equation $Y_{\mathrm{sam}} = Y_{\mathrm{sam}}(I_{\mathrm{sam}}A_{\mathrm{sta}}/I_{\mathrm{sta}}A_{\mathrm{sam}})$, in which A is the absorption intensity and I is integral fluorescence intensity. The quantum yield of quinine bisulfate is 54.6% [31]. By measuring the luminescence of both terbium and cerium, for $LaF_3:Ce^{3+}$, Tb^{3+} NCs dispersed in water, a quantum yield of 19% was found, after coating with the LaF_3 shells, the quantum yield increases to 27%, which is also much higher than that of the $LaF_3:Ce^{3+}$, Tb^{3+} NCs in menthol and water reported previously [9,15].

In general, unlike molecular lanthanide complex compounds, the lanthanide-doped NCs provide a rigid crystal environment, resulting in a higher luminescence quantum yield of the latter. However, the quantum yield of the lanthanide-doped NCs is usually lower than that of the corresponding bulk material. This phenomenon is probably ascribed to the energy-transfer processes to the surface through adjacent dopant ions or the luminescence quenching of the surface dopant ions [16]. If one were able to grow a shell of an un-doped material around each doped nanoparticle, the quench processes could be suppressed. Usually, such passivating shell is made up of a material through which energy cannot be transferred. In recent literatures, different passivating inorganic shells, such as LaF_3 [17,25], $LaPO_4$ [16,28], and $NaYF_4$ [22] have been used to improve the fluorescence of lanthanide-doped materials. In this paper, a facile and effective method is exhibited to grow LaF_3 shell onto $LaF_3:Ln^{3+}$ NCs, resulting in a significant improvement of the luminescence quantum efficiency. The mechanism of such passivating effects can be concluded as the follow facts. Firstly, a significant amount of nonradiative centers existing on the surface of the lanthanide-doped NCs are eliminated by the shielding effect of the passivating shells [16]. Secondly, in the core/shell structures, distances between luminescent lanthanide ions and surface quenchers are increased, thus reducing the nonradiative pathways and suppressing the energy quenching in the energy-transfer processes [17]. Especially, as the $LaF_3:Ln^{3+}$ NCs here are directly prepared in water, their surface may be covered by a large number of O–H groups, which usually cause remarkably non-radiative transition [15]. After passivating shells coated, surface luminescent centers were protected from water, and brighter fluorescence was obtained [18]. Similar effect has been observed in the annealed NdF_3/SiO_2 core/shell nanoparticles reported by our group very recently [32].

Near-Infrared (NIR) radiation in the spectral range 700–1100 nm is referred to as the 'optical window' of cells and tissues owing to the lack of efficient endogenous absorbers there [33]. Nd^{3+} ions with both fluorescence emission and excitation in the NIR region can have desirable use as bio-label, especially in tissue studies. Herein, the $LaF_3:Nd^{3+}$ and the $LaF_3:Nd^{3+}/LaF_3$ core/shell NCs were also prepared, and their luminescent properties were studied. Fig. 5 gives the excitation (monitored at 1056 nm) and emission (excited at 800 nm) spectra of the $LaF_3:Nd^{3+}$ and $LaF_3:Nd^{3+}/LaF_3$ NCs in aqueous solution. Excitation peaks at around 730, 800 and 860 nm correspond to the $^4S_{3/2}/^4F_{7/2}$, $^2H_{9/2}/^4F_{5/2}$ and $^4F_{3/2}$ multiplets of Nd^{3+}, respectively [32,34]. Excited at 800 nm, the emission spectra show typical emission at around 1056 nm corresponding to the $^4F_{3/2} \rightarrow {}^4I_{11/2}$ transitions of Nd^{3+} [12]. It is interesting that all the excitation and emission peaks are within the NIR region, so they can provide both deeper penetration of photons from the excitation source and greater escape depths for the emission signal in biomedical samples. On the other hand, the relatively low emission intensity is observed in $LaF_3:Nd^{3+}$ NCs before being coated with the LaF_3 shell, while the emission of $LaF_3:Nd^{3+}/LaF_3$ NCs was increased by about 60% at 1056 nm. The results indicate that our method was a universal and effective solution to eliminate the surface quenching centers and improve luminescent properties of $LaF_3:Ln^{3+}$ NCs.

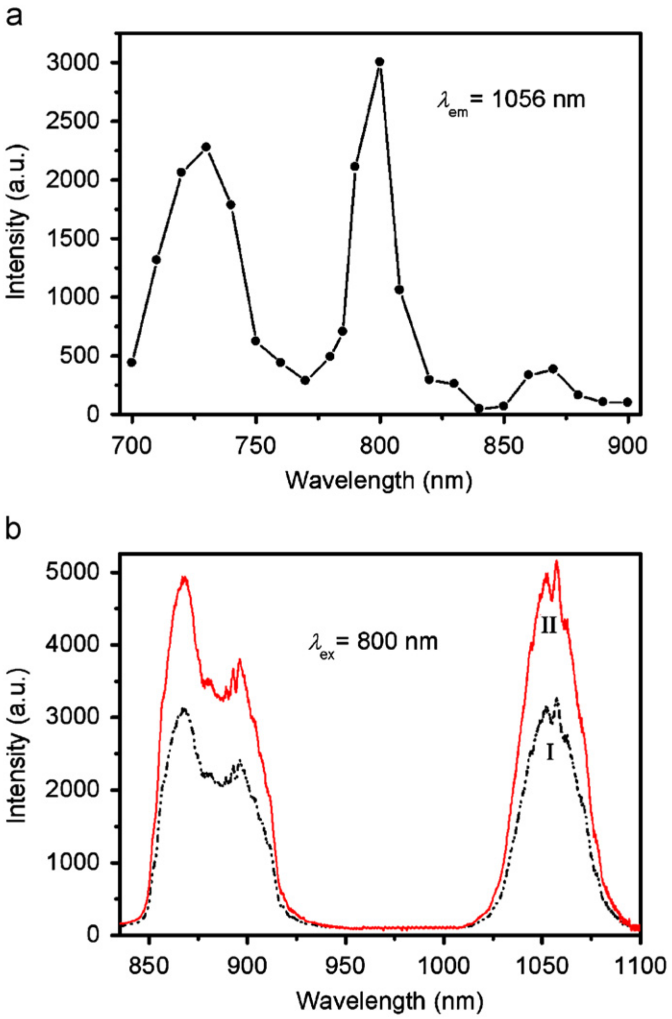

Fig. 5. (a) Excitation ($\lambda_{\mathrm{em}} = 1056$ nm) spectra of $LaF_3:Nd^{3+}/LaF_3$ core/shell NCs; (b) emission ($\lambda_{\mathrm{ex}} = 800$ nm) spectra of $LaF_3:Nd^{3+}$ (I) and $LaF_3:Nd^{3+}/LaF_3$ core/shell NCs (II).

4. Conclusion

In summary, both single-crystalline $LaF_3:Ce^{3+}$, Tb^{3+}/LaF_3 and $LaF_3:Nd^{3+}/LaF_3$ core/shell NCs with hexagonal structure have been successfully synthesized. The core/shell NCs exhibit highly increased emission intensity and quantum yield as compared with the bare LaF_3:Ln^{3+} NCs. This facile method can provide more desirable lanthanide-doped NCs with highly fluorescent properties, which can have potential use in biological areas.

References

[1] A. Mews, A. Eychmuller, M. Giersig, D. Schoos, H. Weller, J. Phys. Chem. 98 (1994) 934.
[2] M. Hines, P. Guyot-Sionnest, J. Phys. Chem. 100 (1996) 468.
[3] X. Gao, Y. Cui, R.M. Levenson, L.W. Chung, S. Nie, Nat. Biotechnol. 22 (2004) 969.
[4] S. Kim, Y.T. Lim, E.G. Soltesz, A.M. Grand, J. Lee, A. Nakayama, J.A. Parker, T. Mihaljevic, R.G. Laurence, D.M. Dor, L.H. Cohn, M.G. Bawendi, J.V. Frangioni, Nat. Biotechnol. 22 (2004) 93.
[5] X.F. Yu, L.D. Chen, K.Y. Li, Y. Li, S. Xiao, X. Luo, J. Liu, L. Zhou, Y.L. Deng, D.W. Pang, Q.Q. Wang, J. Biomed. Opt. 12 (2007) 014008.
[6] S. Xiao, H. Gong, X. Su, J. Han, Y. Han, M. Chen, Q. Wang, J. Phys. Chem. C 111 (2007) 10185.
[7] L. Liu, G. Wei, Z. Liu, Z. He, S. Xiao, Q. Wang, Bioconj. Chem. 19 (2008) 574.
[8] A.M. Derfus, W.C.W. Chan, S.N. Bhatia, NanoLetters 4 (2004) 11.
[9] J.W. Stouwdam, G.A. Hebbink, J. Huskens, F.C.J.M. van Veggel, Chem. Mater. 15 (2003) 4604.
[10] E. Beaurepaire, V. Buissette, M.P. Sauviat, D. Giaume, K. Lahlil, A. Mercuri, D. Casanova, A. Huignard, J.L. Martin, T. Gacoin, J.P. Boilot, A. Alexandrou, NanoLetters 4 (2004) 2079.
[11] H. Deng, S. Yang, S. Xiao, H.M. Gong, Q.Q. Wang, J. Am. Chem. Soc. 130 (2008) 2032.
[12] J.W. Stouwdam, F.C.J.M. van Veggel, NanoLetters 2 (2002) 733.
[13] S. Heer, K. Kömpe, H.U. Gudel, M. Haase, Adv. Mater. 16 (2004) 2102.
[14] J.C. Boyer, F. Vetrone, L.A. Cuccia, J.A. Capobianco, J. Am. Chem. Soc. 128 (2006) 7444.
[15] F. Wang, Y. Zhang, X. Fan, M. Wang, J. Mater. Chem. 16 (2006) 1031.
[16] K. Kömpe, H. Borchert, J. Storz, A. Lobo, S. Adam, T. Müller, M. Haase, Angew. Chem. Int. Ed. 42 (2003) 5513.
[17] Z.L. Wang, Z.W. Quan, P.Y. Jia, C.K. Lin, Y. Luo, Y. Chen, J. Fang, W. Zhou, C.J. O'Connor, J. Lin, Chem. Mater. 18 (2006) 2030.
[18] W. Bu, Z. Hua, H. Chen, J. Shi, J. Phys. Chem. B 109 (2005) 14461.
[19] Y.P. Fang, A.W. Xu, W.F. Dong, Small 1 (2005) 967.
[20] J. Boyer, J. Gagnon, L.A. Cuccia, J.A. Capobianco, Chem. Mater. 19 (2007) 3358.
[21] J.R. DiMaio, B. Kokuoz, T.L. James, J. Ballato, Adv. Mater. 19 (2007) 3266.
[22] G.S. Yi, G.M. Chow, Chem. Mater. 19 (2007) 341.
[23] S. Sivakumar, F.C.J.M. van Veggel, M. Raudsepp, J. Am. Chem. Soc. 127 (2005) 12464.
[24] V. Buissette, M. Moreau, T. Gacoin, J.-P. Boilot, Adv. Funct. Mater. 16 (2006) 351.
[25] J.W. Stouwdam, F.C.J.M. van Veggel, Langmuir 20 (2004) 11763.
[26] M. Darbandi, T. Nann, Chem. Commun. (2006) 776.
[27] X. Peng, M.C. Schlamp, A.V. Kadavanich, A.P. Alivisatos, J. Am. Chem. Soc. 119 (1997) 7019.
[28] L. Zhu, X. Liu, X. Liu, Q. Li, J. Li, S. Zhang, J. Meng, X. Cao, Nanotechnology 17 (2006) 4217.
[29] M. Yu, J. Lin, J. Fu, H.J. Zhang, Y.C. Han, J. Mater. Chem. 13 (2003) 1413.
[30] J.N. Demas, G.A. Crosby, J. Phys. Chem. 75 (1971) 991.
[31] W.H. Melhuish, J. Phys. Chem. 65 (1961) 229.
[32] X.-F. Yu, L.-D. Chen, M. Li, M.-Y. Xie, L. Zhou, Y. Li, Q.-Q. Wang, Adv. Mater. 20 (2008) 4118.
[33] N.W.S. Kam, M. O'Connell, J.A. Wisdom, H. Dai, Proc. Natl. Acad. Sci. 102 (2005) 11600.
[34] C.M. Bender, J.M. Burlitch, Chem. Mater. 12 (2000) 1969.